Molecular Therapy
Methods & Clinical Development
Original Article

A consolidated AAV system for single-cut CRISPR correction of a common Duchenne muscular dystrophy mutation

Yu Zhang,[1,2] Takahiko Nishiyama,[1,2] Hui Li,[1,2] Jian Huang,[3] Ayhan Atmanli,[1,2] Efrain Sanchez-Ortiz,[1,2] Zhaoning Wang,[1,2] Alex A. Mireault,[1,2] Pradeep P.A. Mammen,[2,3] Rhonda Bassel-Duby,[1,2] and Eric N. Olson[1,2]

[1]Department of Molecular Biology, University of Texas Southwestern Medical Center, Dallas, TX 75390, USA; [2]Senator Paul D. Wellstone Muscular Dystrophy Specialized Research Center, University of Texas Southwestern Medical Center, Dallas, TX 75390, USA; [3]Department of Internal Medicine, University of Texas Southwestern Medical Center, Dallas, TX 75390, USA

Duchenne muscular dystrophy (DMD), caused by mutations in the X-linked dystrophin gene, is a lethal neuromuscular disease. Correction of DMD mutations in animal models has been achieved by CRISPR/Cas9 genome editing using *Streptococcus pyogenes* Cas9 (*Sp*Cas9) delivered by adeno-associated virus (AAV). However, due to the limited viral packaging capacity of AAV, two AAV vectors are required to deliver the *Sp*Cas9 nuclease and its single guide RNA (sgRNA), impeding its therapeutic application. We devised an efficient single-cut gene-editing method using a compact *Staphylococcus aureus* Cas9 (*Sa*Cas9) to restore the open reading frame of exon 51, the most commonly affected out-of-frame exon in DMD. Editing of exon 51 in cardiomyocytes derived from human induced pluripotent stem cells revealed a strong preference for exon reframing via a two-nucleotide deletion. We adapted this system to express *Sa*Cas9 and sgRNA from a single AAV9 vector. Systemic delivery of this All-In-One AAV9 system restored dystrophin expression and improved muscle contractility in a mouse model of DMD with exon 50 deletion. These findings demonstrate the effectiveness of CRISPR/*Sa*Cas9 delivered by a consolidated AAV delivery system in the correction of DMD *in vivo*, representing a promising therapeutic approach to correct the genetic causes of DMD.

INTRODUCTION

Duchenne muscular dystrophy (DMD) is a lethal muscle disorder caused by mutations in the *DMD* gene residing on the X chromosome.[1,2] The *DMD* gene encodes the dystrophin protein, which is a large cytoskeletal protein essential for tethering the intracellular actin cytoskeleton and extracellular laminin.[3,4] Absence of dystrophin protein in striated muscles causes skeletal muscle degeneration and myocardial fibrosis, and ultimately progresses to fatal respiratory and cardiac failure. With no transformative treatment available, there is an urgent need to develop new therapeutic approaches for DMD.

Genome editing by clustered regularly interspaced short palindromic repeats (CRISPR) and CRISPR-associated proteins (CRISPR-Cas) represents a promising technology to correct disease-causing mutations in the genome.[5–7] With this approach, Cas9 nuclease is directed by a sequence-specific single guide RNA (sgRNA) to the genome, where it can induce double-stranded breaks (DSBs). In the absence of a repair template, DNA DSBs are repaired by two distinct repair pathways, which are nonhomologous end joining (NHEJ) when there is no sequence microhomology present at the breakage point or microhomology-mediated end joining (MMEJ) when there are 2–25 base pairs (bp) of microhomology on each side of the DSB.[8,9]

Recent studies by our group and others explored the potential of CRISPR-Cas9 gene editing and the NHEJ DNA repair pathway as a means of correcting diverse DMD mutations *in vivo*.[10–21] In mice, sustained dystrophin expression and functional improvement can be observed for at least 12–18 months after systemic delivery of CRISPR-Cas9 genome-editing components by AAV.[13,18] Nevertheless, challenges remain for therapeutic adaptation of CRISPR-Cas9-mediated gene editing for correction of DMD. For example, the limited packaging capacity of AAV requires a dual system consisting of two AAV vectors to separately package *Streptococcus pyogenes* Cas9 (*Sp*Cas9) and sgRNA. In contrast to *Sp*Cas9, the Cas9 ortholog from *Staphylococcus aureus* (*Sa*Cas9) is small enough to be co-packaged with sgRNA into a single AAV vector. However, all current *Sa*Cas9-based genome-editing systems have used a pair of sgRNAs to induce two DNA DSBs flanking the mutated dystrophin exon.[12,13,17–19] This "double-cut" strategy has been reported to introduce additional unwanted genomic modifications, including inversions and AAV integration.[18,22] Moreover, if one DNA DSB is rejoined by NHEJ repair before the initiation of the second DNA DSB, the mutant exon cannot be excised, rendering this double-cut strategy ineffective.

Received 19 March 2021; accepted 28 May 2021;
https://doi.org/10.1016/j.omtm.2021.05.014.

Correspondence: Eric N. Olson, Department of Molecular Biology, University of Texas Southwestern Medical Center, Dallas, TX 75390, USA.
E-mail: eric.olson@utsouthwestern.edu

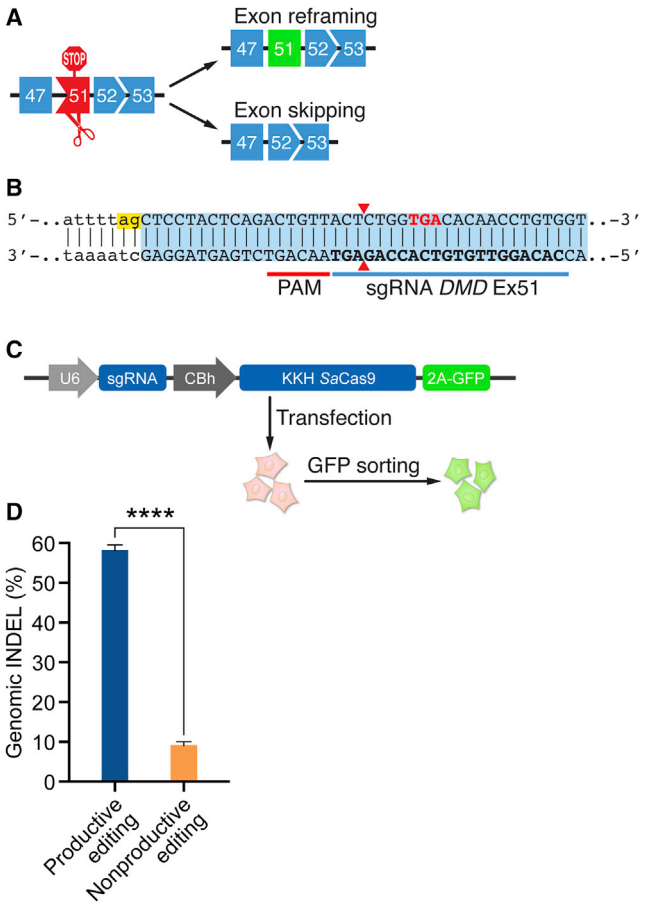

Figure 1. Strategies for CRISPR KKH *Sa*Cas9-mediated gene editing of human *DMD* exon 51

(A) An out-of-frame deletion of human *DMD* exons 48 to 50 (ΔEx48–50) results in splicing of exons 47 to 51, generating a premature termination codon in exon 51. A single-cut editing strategy was designed to enable CRISPR-KKH *Sa*Cas9 DNA cutting to restore the open reading frame of the *DMD* gene. Small insertions and deletions (indels) with two nucleotide deletions (3n-2) can reframe exon 51. Large indels disrupting the 5′-AG-3′ splice acceptor sequence cause exon 51 skipping, resulting in splicing of exon 47 to exon 52. (B) Illustration of the sgRNA targeting human *DMD* exon 51. This sgRNA recognizes a 5′-AACAGT-3′ PAM in exon 51 and generates a DSB 4 bp upstream of the 5′-TGA-3′ premature termination sequence (indicated in red). The 5′-AG-3′ splice acceptor sequence is indicated in yellow. (C) Illustration of a plasmid-encoding KKH *Sa*Cas9 with 2A-GFP, driven by a hybrid form of cytomegalovirus and chicken beta-actin promoter (CBh). The plasmid also encodes a sgRNA driven by the U6 promoter. Cells transfected with this plasmid express GFP, allowing for selection of KKH *Sa*Cas9-expressing cells by FACS. (D) Analysis of genomic indels in KKH *Sa*Cas9-edited *DMD* ΔEx48–50 iPSCs. Productive editing is defined as indels with 3n-2 deletion, which are capable of reframing or skipping exon 51. Data are represented as mean ± SEM. Unpaired two-tailed Student's t tests was performed. *p < 0.05 (n = 3).

In this study, we explored the potential of CRISPR-E782K/N968K/R1015H (CRISPR-KKH) *Sa*Cas9-mediated single-cut gene editing as a means of correcting an exon 50 DMD deletion mutation. KKH *Sa*Cas9 is a *Sa*Cas9 variant carrying three amino acid substitutions in the protospacer-adjacent motif (PAM)-interacting domain that enable strong genome-editing activities at target sites with a 5′-NNNRRT-3′ PAM.[23] We first performed single-cut gene editing with KKH *Sa*Cas9 in cardiomyocytes derived from human DMD induced pluripotent stem cells (iPSCs) harboring a deletion of exons 48–50 (ΔEx50), the most common "hotspot" region for DMD exon deletions. High frequency of a two-nucleotide deletion was observed after KKH *Sa*Cas9-mediated single-cut gene editing, which restored the open reading frame (ORF) of the dystrophin gene. Next, we packaged KKH *Sa*Cas9 and sgRNA into a single AAV9 vector and performed *in vivo* genome editing of exon 51 in mice with a deletion of *Dmd* exon 50. Systemic delivery of the consolidated CRISPR-KKH *Sa*Cas9 AAV9 vector showed efficient restoration of dystrophin expression in skeletal muscle and heart and improved muscle contractility. These findings show that delivery of KKH-*Sa*Cas9 with a single sgRNA in a single vector system is effective in correcting DMD *in vivo*, representing an important advancement toward potential therapeutic translation.

RESULTS

Strategies for CRISPR-KKH *Sa*Cas9-mediated genome editing of human *DMD* exon 51

The majority of DMD deletion mutations are clustered in hotspot regions, comprised of exons 2–20 and exons 45–55, that disrupt the continuity of the ORF with downstream exons. Exon deletions immediately preceding exon 51, which disrupt the reading frame of this exon, represent the most common type of human DMD mutation.[24] Our ultimate goal was to develop a consolidated AAV expression system encoding SaCas9 and an optimal sgRNA for reframing of exon 51 so as to enable *in vivo* DMD correction with an All-In-One vector. To optimize this gene editing strategy, we used iPSCs generated from DMD patients harboring a deletion of exons 48 to 50 (ΔEx48–50) in the *DMD* gene. This deletion results in splicing of exon 47 to exon 51, which introduces a premature stop codon in exon 51 (Figure 1A).

We did not identify efficient sgRNAs for wild-type (WT) *Sa*Cas9 capable of reframing human *DMD* exon 51, so we considered various *Sa*Cas9 mutants with amino acid substitutions in the PAM-interacting domain that expand the range of DNA cutting by relaxing PAM specificity. From this analysis, we identified a sgRNA for the KKH variant of *Sa*Cas9 that recognizes a 5′-AACAGT-3′ PAM in exon 51 and generates a DNA DSB 4-bp upstream of the premature termination codon (Figure 1B). Depending on the repair outcome, two types of insertions and deletions (indels) could restore the exon 51 ORF. Exon 51 could potentially be reframed through indels that delete two nucleotides (3n-2), or exon 51 could be skipped if the indel is large enough to delete the 5′-AG-3′ splice acceptor (Figure 1A).

The gene-editing efficiency of KKH *Sa*Cas9 was tested by transfecting *DMD* ΔEx48–50 iPSCs with a plasmid expressing KKH *Sa*Cas9 and sgRNA, and gene-edited cells were enriched through fluorescence-activated cell sorting (FACS) (Figure 1C). We performed tracking of indels by decomposition (TIDE) analysis to assess sgRNA cutting efficiency and indel patterns. We found that this sgRNA enabled high

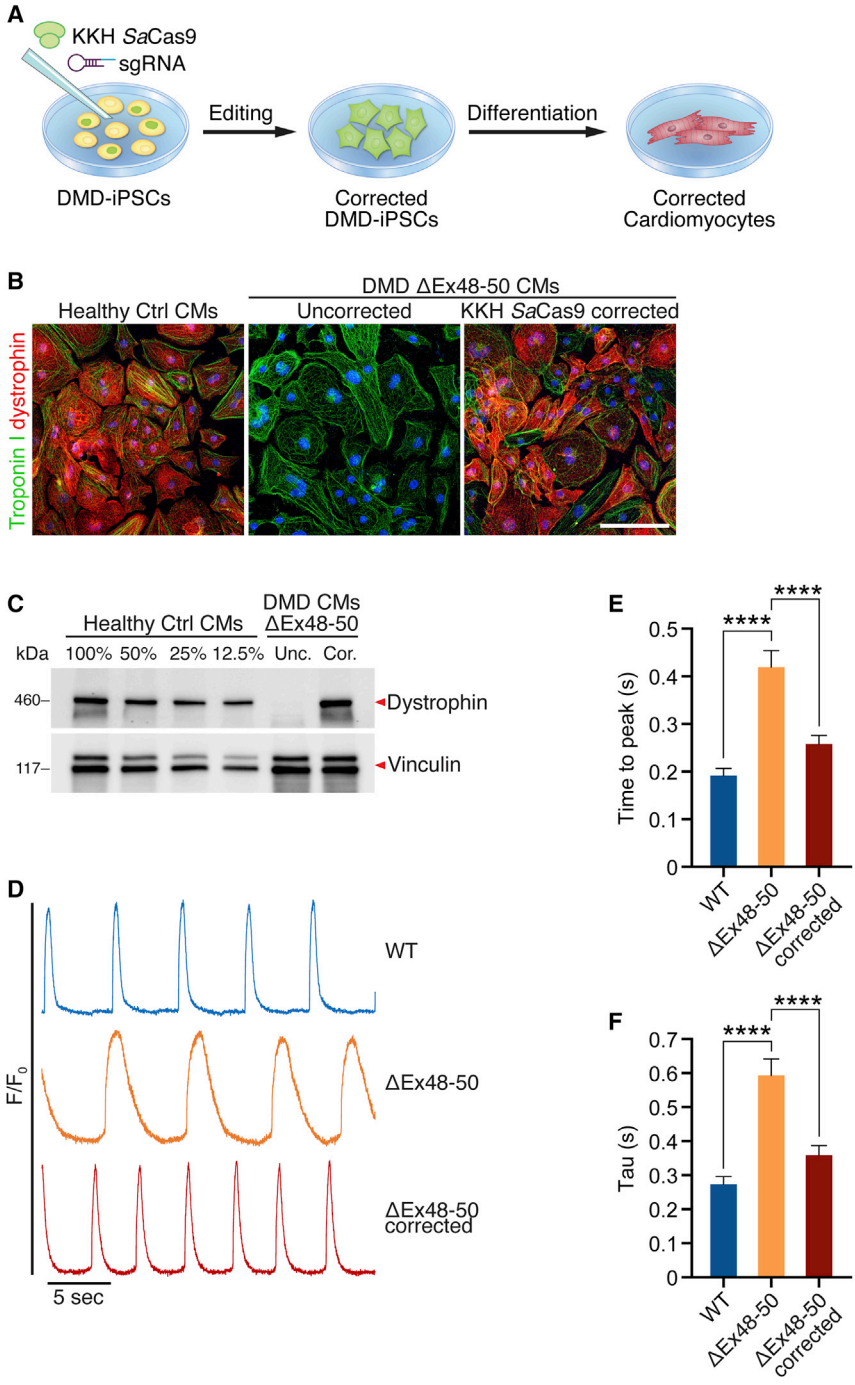

Figure 2. Restoration of dystrophin expression in *DMD* ΔEx48–50 cardiomyocytes after CRISPR-KKH *Sa*Cas9-mediated single-cut gene editing

(A) *DMD* ΔEx48–50 iPSCs were edited by KKH *Sa*Cas9 (corrected DMD iPSCs) and then differentiated into corrected cardiomyocytes (CMs) for downstream analysis. (B) Immunocytochemistry shows dystrophin restoration in mixtures of *DMD* ΔEx48–50 CMs following KKH *Sa*Cas9-mediated single-cut gene editing. Red, dystrophin staining; green, troponin I staining. Scale bar, 100 μm. (C) Western blot shows dystrophin restoration in mixtures of *DMD* ΔEx48–50 CMs following KKH *Sa*Cas9-mediated single-cut gene editing. Dilutions of protein extract from healthy control CMs were used to standardize dystrophin protein expression. Vinculin was used as the loading control. (D) Representative traces of spontaneous calcium activity of iPSC-derived CMs cultured with calcium indicator Fluo-4AM. Traces show change in fluorescence intensity (F) in relationship to resting fluorescence intensity (F_0). (E) Quantification of calcium release phase of contraction, as measured by time to peak, in iPSC-derived CMs. Data are represented as mean ± SEM. One-way ANOVA was performed with post hoc Tukey's multiple-comparisons test. ****$p < 0.0001$ ($n = 40$). (F) Quantification of calcium reuptake phase of contraction, as measured by tau, in iPSC-derived CMs. Data are represented as mean ± SEM. One-way ANOVA was performed with post hoc Tukey's multiple-comparisons test. ****$p < 0.0001$ ($n = 40$).

editing activity of *DMD* exon 51, generating over 65% of total indels (Figure 1D). More than 55% of indels allowed productive editing (3n-2), capable of restoring the *DMD* exon 51 ORF (Figures 1D and S1).

Interestingly, 45% of KKH *Sa*Cas9-induced indels had a deletion of a 5′-CT-3′ dinucleotide, which allows reframing of the *DMD* exon 51 ORF (Figure S1). The sgRNA designed in this study enables the KKH *Sa*Cas9 nuclease to induce a DNA DSB between the 5′-CTCT-3′ tetranucleotide, generating a 2-nt 5′-CT-3′ microhomology on each side of the breakage site (Figure S1), leading to high frequency of precise deletion of the 5′-CT-3′ dinucleotide. These data demonstrate that KKH *Sa*Cas9-mediated single-cut gene editing is an efficient and practicable strategy to restore the dystrophin ORF in *DMD* exon 51, caused by deletion of preceding exons.

CRISPR-KKH *Sa*Cas9-mediated single-cut gene editing restores dystrophin expression in *DMD* ΔEx48–50 iPSC-derived cardiomyocytes

Human iPSCs generated from a ΔEx48–50 DMD patient were corrected by KKH *Sa*Cas9 and sgRNA using the single-cut gene-editing approach and then differentiated to cardiomyocytes (iPSC-CMs) (Figure 2A). The mutation in uncorrected *DMD* ΔEx48–50 iPSC-CMs results in a premature termination codon following the first eight amino acids encoded by exon 51 (Figure S2). Correction of *DMD* ΔEx48–50 iPSC-CMs was accomplished by reframing of the *DMD* gene, as assessed by reverse transcription PCR (RT-PCR) and sequencing using a forward primer targeting exon 47 and a reverse primer targeting exon 52. Corrected *DMD* ΔEx48–50 iPSC-CMs had a deletion of the 5′-CT-3′

dinucleotide, which reframed exon 51 (Figure S2). We confirmed restoration of dystrophin protein expression by immunocytochemistry and western blot analysis (Figures 2B and 2C). Even without clonal selection and expansion, cardiomyocytes differentiated from KKH *Sa*Cas9-edited *DMD* ΔEx48–50 iPSC mixtures showed a high level of dystrophin protein comparable to healthy control iPSC-CMs (Figures 2B and 2C).

Dysregulation of calcium handling is a common pathogenic phenotype seen in DMD cardiomyocytes. To assess the consequences of the *DMD* ΔEx48–50 mutation and the effect of gene editing by the KKH *Sa*Cas9-mediated single-cut strategy, we analyzed spontaneous calcium activity in healthy control and *DMD* ΔEx48–50 iPSC-CMs (Figure 2D). Calcium transient kinetics, including time to peak and decay rate, were abnormally elevated in uncorrected *DMD* ΔEx48–50 iPSC-CMs (Figures 2E and 2F). After KKH *Sa*Cas9 gene editing, *DMD* ΔEx48–50 iPSC-CMs displayed normal calcium transient kinetics similar to healthy control iPSC-CMs (Figures 2E and 2F), indicating restoration of calcium release and reuptake. Next, we performed genotoxicity analysis in KKH *Sa*Cas9-edited *DMD* ΔEx48–50 iPSC-CMs. We did not observe significant genomic editing at the top eight predicted off-target sites (Figure S3). Therefore, KKH *Sa*Cas9-mediated single-cut gene editing represents an efficient and safe strategy to restore the ORF of human *DMD* exon 51 caused by exon 50 deletion, thereby allowing functional restoration in gene-edited DMD iPSC-CMs.

Systemic delivery of All-In-One AAV-packaged CRISPR-KKH *Sa*Cas9 restores dystrophin expression in ΔEx50 mice

To further evaluate the efficacy of CRISPR-KKH *Sa*Cas9 gene editing *in vivo*, we packaged the KKH *Sa*Cas9 nuclease and its sgRNA in one AAV vector (Figure 3A). In this All-In-One AAV system, KKH *Sa*Cas9 expression was driven by a muscle-specific Creatine Kinase 8 (CK8) promoter, restricting its expression to skeletal muscles and heart.[25] Because the sgRNA is rate limiting for *in vivo* gene editing of DMD mouse models,[13,16] we included two copies of an expression cassette encoding the same sgRNA (targeting mouse *Dmd* exon 51) driven by two RNA polymerase III promoters, 7SK and U6, in this All-In-One AAV system (Figure 3A).

Postnatal day 4 (P4) DMD mice with exon 50 deletion (ΔEx50) were injected intraperitoneally (i.p.) with All-In-One AAV-packaged KKH *Sa*Cas9 at two different doses, 2×10^{14} vector genomes (vg)/kg (low dose) and 4×10^{14} vg/kg (high dose) (Figure 3B). Four weeks after systemic AAV delivery, the skeletal muscles and heart of KKH *Sa*Cas9-edited ΔEx50 mice were harvested for analysis. Assessment by immunohistochemistry showed that dystrophin restoration in skeletal muscles was dose dependent (Figures 3C, S4, and S5). ΔEx50 mice receiving the low-dose All-In-One AAV treatment displayed 36% and 52% dystrophin-positive myofibers in tibialis anterior (TA) and triceps muscles, respectively (Figure S5). With low-dose All-In-One AAV treatment, the diaphragm showed higher percentages of dystrophin-positive myofibers, reaching 79% (Figure S5). When the dose of All-In-One AAV was increased to 4×10^{14} vg/kg, a substantial increase of dystrophin-positive myofibers in TA and triceps was observed (Figure S5).

Next, we performed western blot analysis to quantitatively assess dystrophin restoration in skeletal muscles and heart after systematic delivery of All-In-One AAV-packaged KKH *Sa*Cas9 and sgRNA. ΔEx50 mice receiving the low-dose All-In-One AAV restored 12% and 26% of dystrophin protein in TA and triceps, respectively (Figures 4A and 4B). When the dose of All-In-One AAV was increased to 4×10^{14} vg/kg, dystrophin protein restoration in TA and triceps was over 27%. Dystrophin protein expression in the diaphragm and heart exceeded 45% and 38%, respectively, even at the low dose of All-In-One AAV treatment (Figures 4A and 4B), indicating that dystrophin protein restoration in the diaphragm and heart is greater than in TA and triceps.

To quantify *in vivo* gene-editing efficiency in ΔEx50 mice, we performed deep-sequencing analysis to determine the indel frequency and pattern at the genomic level. ΔEx50 mice treated with low-dose All-In-One AAV had an average of 4%–10% of total indels in skeletal muscles and heart; the total indels in the high-dose group increased to 8%–12% (Figure 4C). Notably, a −2-nt deletion, which is capable of reframing the *Dmd* exon 51 ORF, was the predominant indel in the All-In-One AAV-treated ΔEx50 mice. These findings indicate that KKH *Sa*Cas9-mediated single-cut gene editing coupled with the single vector delivery system can effectively correct DMD mutations *in vivo*.

Systemic delivery of All-In-One AAV-packaged CRISPR-KKH *Sa*Cas9 restores muscle integrity and improves muscle function in ΔEx50 mice

To evaluate whether systemic delivery of All-In-One AAV-packaged KKH *Sa*Cas9 was able to rescue pathological phenotypes seen in dystrophic mice, we performed hematoxylin and eosin (H&E) (Figures S6 and S7) and Masson's trichrome staining (Figures S9 and S10) of skeletal muscles and heart isolated from ΔEx50 mice 4 weeks after KKH *Sa*Cas9-mediated gene editing. Skeletal muscles from ΔEx50 mice without gene editing displayed necrosis and inflammatory infiltration (Figures S6 and S7). The percentage of regenerating myofibers with central nuclei in untreated ΔEx50 mice was between 25% and 35% across different skeletal muscle groups (Figures S8A–S8C). After All-In-One AAV treatment, the percentage of centrally nucleated myofibers declined substantially (Figures S8A–S8C). Distribution of myofiber cross-sectional area also showed an improvement in the TA muscle after delivery of All-In-One AAV at both doses (Figure S8D). Masson's trichrome staining showed substantial fibrosis and necrosis in untreated ΔEx50 mice (Figures S9 and S10), ranging between 10% and 15% across different skeletal muscle groups (Figures S11A–S11C). After All-In-One AAV treatment, the percentage of fibrotic and necrotic area dramatically declined (Figures S9–S11).

To examine the effect of gene editing on muscle function, we performed grip-strength analysis on ΔEx50 mice at 4 weeks after

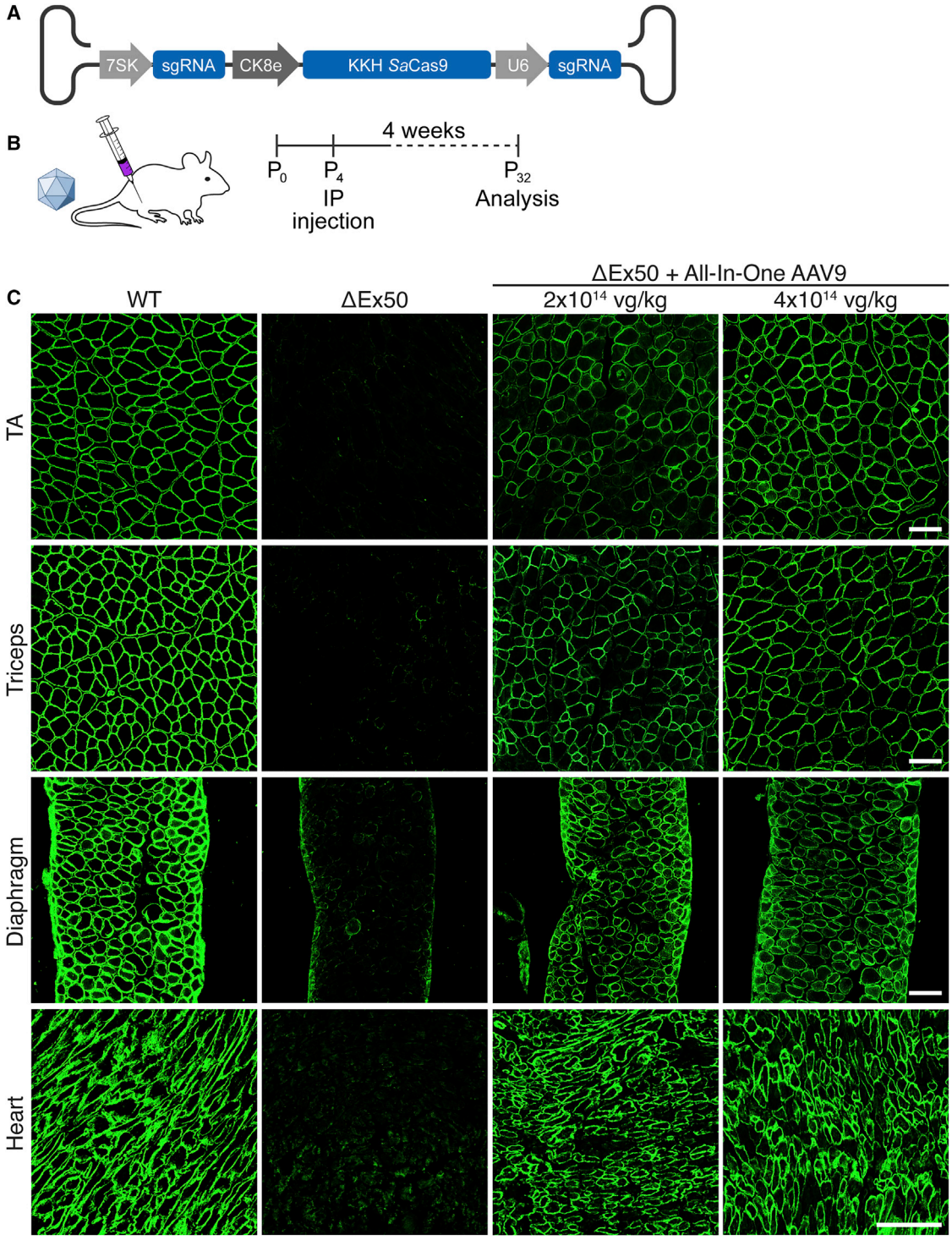

Figure 3. Systemic delivery of All-In-One AAV-packaged KKH *Sa*Cas9 restores dystrophin expression in ΔEx50 mice

(A) Illustration of the All-In-One AAV vector used to deliver KKH *Sa*Cas9 gene-editing components. KKH *Sa*Cas9 expression is driven by a muscle-specific CK8 promoter. Two copies of the same sgRNA targeting mouse *Dmd* exon 51 are driven by two RNA polymerase III promoters, 7SK and U6. (B) Illustration of systemic delivery of All-In-One AAV vectors in ΔEx50 mice. Postnatal day 4 ΔEx50 mice were injected intraperitoneally with 2×10^{14} or 4×10^{14} vg/kg of All-In-One AAV vectors. Four weeks after systemic delivery, ΔEx50 mice and WT littermates were dissected for analysis. (C) Immunohistochemistry shows restoration of dystrophin in the tibialis anterior (TA), triceps, diaphragm, and heart of ΔEx50 mice 4 weeks after systemic delivery of AAV-packaged KKH *Sa*Cas9 and sgRNA. Dystrophin is shown in green. n = 6 for each muscle group. Scale bars, 100 μm.

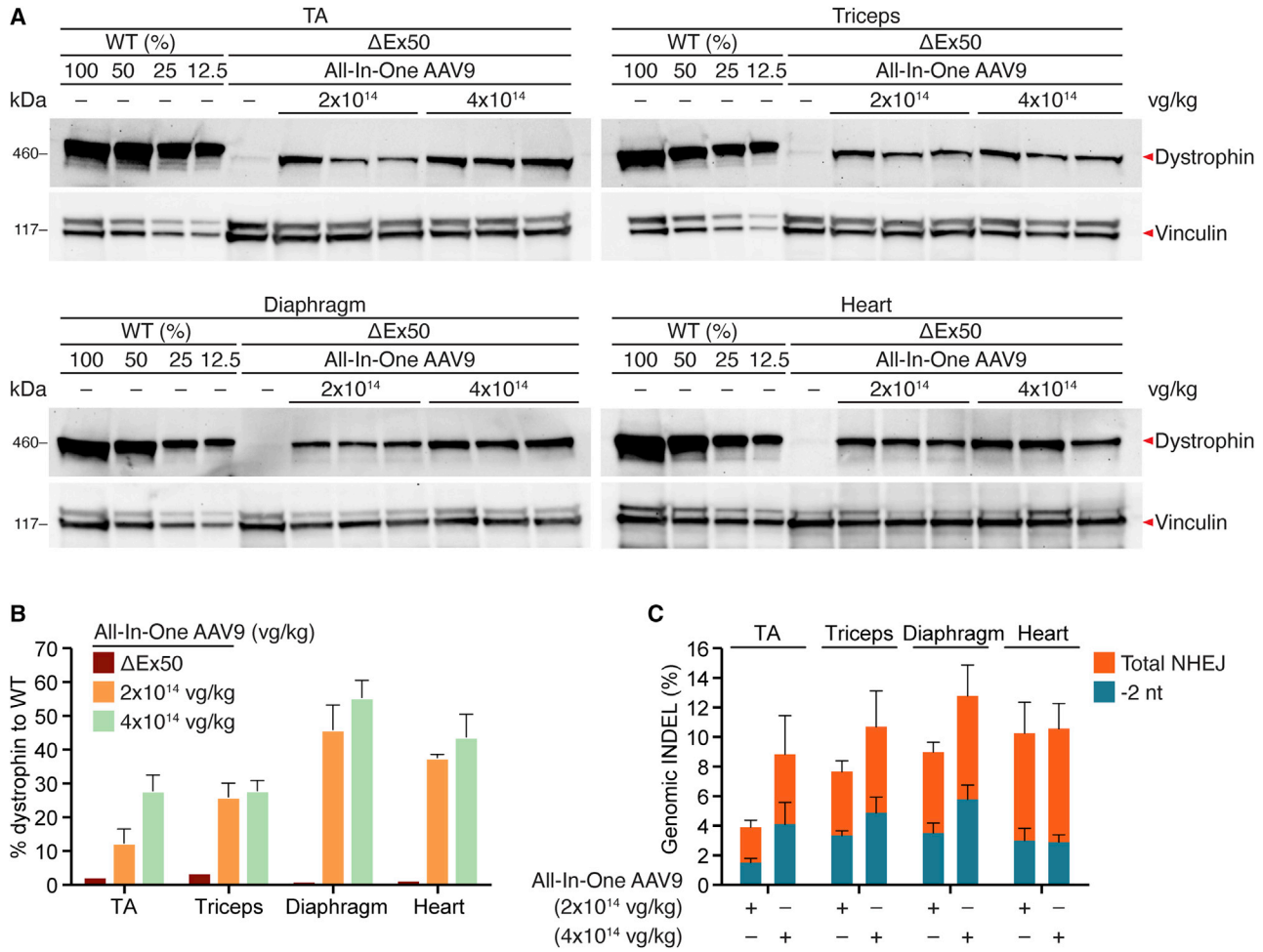

Figure 4. Western blot and genomic analysis of skeletal muscles and heart of ΔEx50 mice receiving systemic All-In-One AAV delivery of KKH *Sa*Cas9 gene-editing components

(A) Western blot analysis shows restoration of dystrophin expression in the TA, triceps, diaphragm, and heart of ΔEx50 mice 4 weeks after systemic delivery of All-In-One AAV-packaged KKH *Sa*Cas9 and sgRNA. The dose of the AAV vector is indicated. Dilutions of protein extract from WT mice were used to standardize dystrophin protein expression. Vinculin was used as the loading control (n = 3 for each dose). (B) Quantification of dystrophin expression in the TA, triceps, diaphragm, and heart. Relative dystrophin intensity was calibrated with vinculin internal control before normalizing to the WT control. (C) Genomic indel quantification by deep-sequencing analysis of the TA, triceps, diaphragm, and heart of ΔEx50 mice 4 weeks after systemic delivery of All-In-One AAV-packaged KKH *Sa*Cas9 and sgRNA. Data are represented as mean ± SEM.

systemic All-In-One AAV delivery. ΔEx50 mice without gene editing showed a 56% and 45% reduction of grip strength in forelimb and hindlimb compared to the WT littermates, respectively (Figure S12). Forelimb and hindlimb grip strength of ΔEx50 mice receiving low-dose All-In-One AAV treatment showed a trend toward improvement (Figure S12). Moreover, ΔEx50 mice receiving high-dose All-In-One AAV treatment showed a dramatic improvement of forelimb and hindlimb grip strength by 86% and 67%, respectively, compared to the untreated ΔEx50 littermates (Figure S12). In addition, we also performed electrophysiological analysis on soleus and extensor digitorum longus (EDL) muscles isolated from ΔEx50 mice at 4 weeks after receiving the high-dose All-In-One AAV treatment. We observed rescue of specific force and maximal tetanic force in the soleus and EDL muscle of the corrected ΔEx50 mice (Figures 5A–5D). Without KKH *Sa*Cas9 gene editing, muscle force was reduced by 30% in slow-twitch soleus muscle and 69% in fast-twitch EDL muscle compared to the WT littermates (Figures 5A and 5B). After systemic delivery of All-In-One AAV-packaged KKH *Sa*Cas9, muscle-specific force of the soleus and EDL was increased by 51% and 78%, respectively, compared to the untreated ΔEx50 littermates (Figures 5A and 5B). The maximal tetanic force of the soleus and EDL also followed a similar pattern as seen for specific force (Figures 5C and 5D).

Next, we performed fatigue analysis in WT and ΔEx50 mice. Without KKH *Sa*Cas9 gene editing, ΔEx50 mice exhibited faster force reduction in soleus and EDL. The average time for 50% force reduction in soleus and EDL from ΔEx50 mice was reduced by 38% and 29%, respectively, compared to the WT littermates (Figures 5E and 5F).

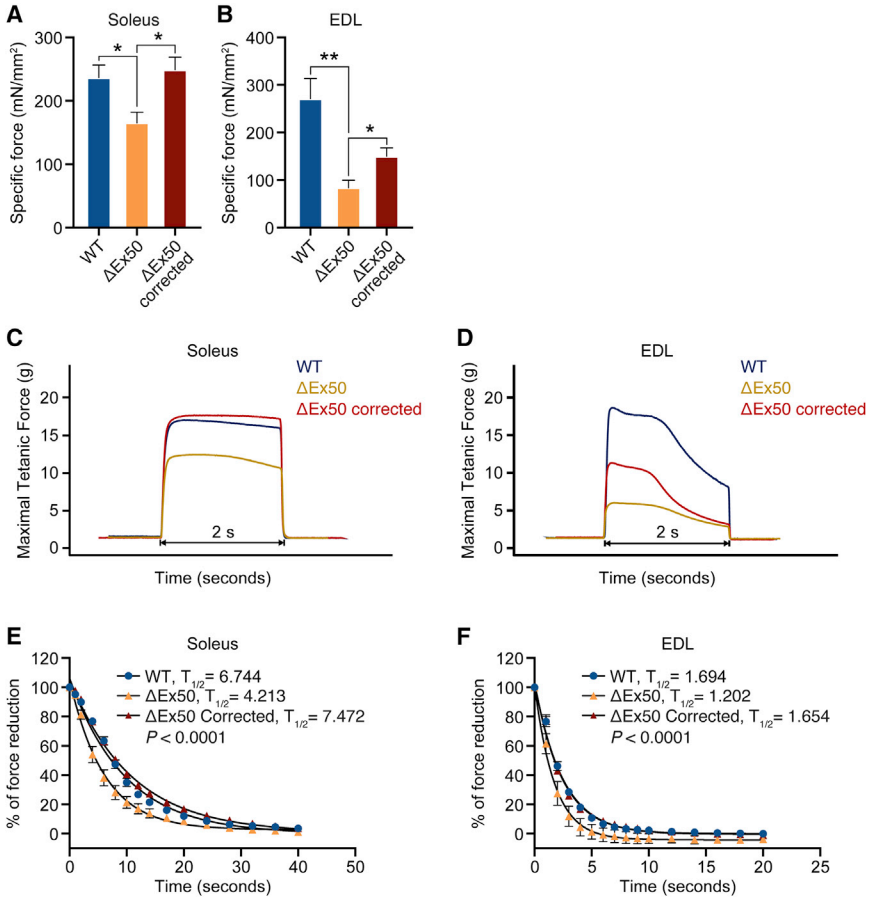

Figure 5. Systemic delivery of All-In-One AAV-packaged CRISPR-KKH *Sa*Cas9 improves muscle function in ΔEx50 mice

(A and B) Specific force (mN/mm^2) of the soleus (A) and extensor digitorum longus (EDL) (B) in WT, ΔEx50 mice untreated, and ΔEx50 mice treated with All-In-One AAV-packaged KKH *Sa*Cas9. Data are represented as mean ± SEM. Brown-Forsythe and Welch ANOVA test was performed. *p < 0.05, **p < 0.005 (n = 6). (C and D) Maximal tetanic force of the soleus (C) and EDL (D) in WT, ΔEx50 mice untreated, and ΔEx50 mice treated with All-In-One AAV-packaged KKH *Sa*Cas9. (E and F) Fatigue resistance analysis of soleus (E) and EDL (F) in WT, ΔEx50 mice untreated, and ΔEx50 mice treated with All-In-One AAV-packaged KKH *Sa*Cas9. Data are represented as mean ± SEM. Nonlinear regression with extra sum-of-squares F test was performed (n = 6).

After KKH *Sa*Cas9-mediated gene editing, the force reduction rate of soleus and EDL from ΔEx50 mice was restored to the WT level (Figures 5E and 5F), indicating enhanced fatigue resistance. Improvement of muscle function correlated with increased dystrophin expression and decreased muscle degeneration (Figure S13).

Elevated serum creatine kinase (CK) is a pathological hallmark of DMD. After receiving the low- and high-dose All-In-One AAV treatment, CK levels in the ΔEx50 mice were reduced by 66% and 81%, respectively, compared to the untreated ΔEx50 littermates (Figure S14). Together, these findings demonstrate that KKH *Sa*Cas9-mediated single-cut gene editing improves muscle integrity and provides functional benefit to DMD ΔEx50 mice.

DISCUSSION

Despite intense efforts to develop therapeutic strategies to restore dystrophin expression in DMD patients through oligonucleotide-mediated exon skipping and gene therapy with truncated forms of dystrophin, there remains a major unmet need for approaches to restore maximal portions of the dystrophin gene in patients with different DMD deletions.[26–28] Exon deletions that disrupt the continuity of the dystrophin ORF in exon 51 represent the most predominant cause of DMD. Skipping or reframing exon 51, in principle, can provide therapeutic benefit to ~13% of the DMD population.[24] To date, there is no report of using *Sa*Cas9-mediated single-cut gene editing to correct DMD mutations. Previously published studies employed two sgRNAs to direct *Sa*Cas9 to induce two DNA DSBs flanking an out-of-frame exon.[12,13,17–19,22]

In this study, we developed a single-cut gene-editing strategy in which KKH *Sa*Cas9 introduces a single DNA DSB within exon 51 to reframe the dystrophin ORF in human cardiomyocytes lacking exons 48–50 and in mouse muscles lacking exon 50. Cardiomyocytes derived from human iPSCs with the ΔEx48–50 mutation and corrected by editing with KKH *Sa*Cas9 restored dystrophin expression and showed improved calcium transient kinetics. We also packaged KKH *Sa*Cas9 and its sgRNA into a single AAV vector and performed *in vivo* gene editing. DMD ΔEx50 mice receiving systemic All-In-One AAV treatment restored dystrophin expression with consequent improvement in muscle contractility and force. This study represents the first application of KKH *Sa*Cas9-mediated single-cut gene editing for the treatment of DMD.

*Sp*Cas9-mediated single-cut gene editing has been widely used for correcting diverse DMD mutations with high efficiency, especially for mutations that can be reframed by a 1-bp insertion.[10,11,15,16,20,21] In contrast, prior studies of *Sa*Cas9-mediated correction of DMD mutations relied on two sgRNAs to completely excise the out-of-frame exon.[12,13,17–19,22] These different approaches are dependent on the topological distinctions between the DNA DSBs induced by *Sp*- and *Sa*Cas9. Studies using molecular dynamics simulations suggest that an *Sp*Cas9-induced DNA DSB generates a staggered cut, producing a single-nucleotide 5′ overhang, leading to a high frequency of a 1-bp insertion after NHEJ-mediated repair.[29,30] In contrast, the DSB generated by *Sa*Cas9 cutting is blunt ended, with indels with varying

lengths. Therefore, NHEJ-mediated 1-bp insertion appears to be an *Sp*Cas9-specific phenomenon, which does not apply to *Sa*Cas9.[31] This distinction poses limitations to *Sa*Cas9-mediated single-cut gene editing as a general strategy for reframing out-of-frame exons. In order to address this issue, we screened for sgRNAs capable of directing KKH *Sa*Cas9 to induce a DNA DSB between a microhomology sequence. Studies have demonstrated that DNA DSBs around regions of microhomology tend to generate deletions with predictable length.[8,31] As expected, with *Sa*Cas9 cutting, we observed a majority of productive editing events containing a precise deletion of the 5′-CT-3′ dinucleotide.

Although CRISPR correction of DMD has shown promise in pre-clinical studies, several questions and challenges remain to be addressed. The first concern is durability of CRISPR gene editing in muscle cells. Skeletal muscle has resident stem cells (satellite cells) capable of regenerating or fusing to myofibers.[32] Although there is increasing evidence that AAV9 delivery of CRISPR-Cas9 components can transduce and edit satellite cells,[19,22,33] the efficiency of viral transduction and gene editing in satellite cells remains low. Whether unedited satellite cells will gradually dilute out corrected nuclei in regenerating myofibers remains unknown. Engineering novel AAV serotypes with strong tropism to satellite cells may offer a potential solution to this issue. Another concern is the AAV dose administered in gene editing. In pre-clinical studies, the average AAV dose used in *in vivo* gene editing of DMD animal models varies between 1.6×10^{14} and 1.8×10^{15} vg/kg,[10–14,16–22] which becomes an obvious burden for industrial production and clinical translation. Similarly, AAV dose of 2.0×10^{14} vg/kg or higher has been necessary to direct therapeutically beneficial levels of micro-dystrophin in early-stage clinical trials.[34]

Self-complementary AAV has been shown to be superior to single-stranded AAV in viral transduction and CRISPR gene editing.[15,20] When self-complementary AAV is used for CRISPR sgRNA delivery, the viral dose can be reduced to 8×10^{13} vg/kg. However, *Sa*Cas9 used in this study is too large to be packaged into self-complementary AAV. Potential solutions to address these concerns include (1) screening more compact CRISPR/Cas systems to bypass the packaging limit of self-complementary AAV and (2) dividing *Sa*Cas9 into two parts to accommodate self-complementary AAV packaging and using the split-intein system to reconstitute the full-length Cas9 after AAV delivery.[35,36]

Although complete restoration of normal levels of dystrophin is not achievable for therapeutic gene editing because AAV viral transduction of skeletal muscles is not 100%, studies in patients with Becker muscular dystrophy have estimated that ~15% of normal levels of dystrophin protein could provide therapeutic benefits.[37] Our *in vivo* data demonstrate that All-In-One *Sa*Cas9-mediated single-cut gene editing has high efficiency in dystrophin restoration, capable of restoring 30%–50% of dystrophin protein levels in multiple skeletal muscles and 50% in the heart within 4 weeks of administration. Therefore, All-In-One *Sa*Cas9-mediated single-cut gene editing developed in this study shows strong potential for therapeutic translation and represents a promising therapy for permanent correction of DMD.

Finally, we have recently reported the effectiveness of base editing as a strategy for exon skipping in DMD via splice-site modification.[38] Whether this approach might be adapted to an All-In-One strategy is under investigation. Together, these various approaches add to the expanding toolbox of gene-editing strategies that may ultimately be applied to different DMD mutations.

MATERIALS AND METHODS

Study design

This study was designed with the primary aim of investigating the feasibility of using CRISPR/*Sa*Cas9-mediated single-cut gene editing for the correction of DMD mutations. The secondary objective was to design an All-In-One AAV packaging system to deliver CRISPR/*Sa*Cas9 and sgRNAs for *in vivo* therapeutic gene editing. We did not use exclusion, randomization, or blind approaches to assign the animals for the experiments. Grip-strength tests, histology validation, immunostaining analysis, CK analysis, and muscle electrophysiology were performed as blinded experiments. For each experiment, sample size reflects the number of independent biological replicates and was provided in the figure legends.

KKH *Sa*Cas9 vector cloning and AAV vector production

WT *Sa*Cas9 complementary DNA (cDNA) was cut from pX601 plasmid,[39] a gift from F. Zhang (Addgene plasmid #61591), using AgeI-HF and BamHI-HF, and subcloned into p*Lb*Cpf1-2A-GFP plasmid by replacing *Lb*Cpf1,[40] generating the p*Sa*Cas9-2A-GFP plasmid. Modified *Sa*Cas9 sgRNA scaffold and KKH *Sa*Cas9 C terminus cDNA (E782K/N968K/R1015H) were synthesized as gBlocks (Integrated DNA Technologies) and subcloned into p*Sa*Cas9-2A-GFP plasmid using an In-Fusion cloning kit (Takara Bio), generating the pKKH-*Sa*Cas9-2A-GFP plasmid. The sgRNAs targeting human *DMD* exon 51 or mouse *Dmd* exon 51 were subcloned into the newly generated pKKH-*Sa*Cas9-2A-GFP plasmid using BbsI digestion and T4 ligation. KKH *Sa*Cas9, 7SK, and U6 sgRNA expression cassettes were subcloned into the pSSV9 single-stranded AAV plasmid using an In-Fusion cloning kit (Takara Bio). Cloning primer sequences are listed in Table S1. AAV viral plasmid was column purified and digested with SmaI and AhdI to check inverted terminal repeat (ITR) integrity. AAV was packaged by Boston Children's Hospital Viral Core, and serotype 9 was chosen for capsid assembly. AAV titer was determined by quantitative real-time PCR assay.

Human iPSC maintenance, nucleofection, and differentiation

DMD ΔEx48–50 iPSCs (RBRC-HPS0164) were purchased from Cell Bank RIKEN BioResource Center. Stem cell work described in this manuscript has been conducted under the oversight of the UT Southwestern Stem Cell Research Oversight (SCRO) Committee. Human iPSCs were cultured in mTeSR plus medium (STEMCELL Technologies) and passaged approximately every 4 days (1:18 split ratio). One hour before nucleofection, iPSCs were treated with 10 μM ROCK

inhibitor (Y-27632) and dissociated into single cells using Accutase (Innovative Cell Technologies). iPSCs (1×10^6) were mixed with 5 μg of the pKKH-*Sa*Cas9-2A-GFP plasmid. The P3 Primary Cell 4D-Nucleofector X kit (Lonza) was used for nucleofection according to the manufacturer's protocol. After nucleofection, iPSCs were cultured in mTeSR plus medium supplemented with 10 μM ROCK inhibitor, and Primocin (100 μg/mL; InvivoGen). Three days after nucleofection, GFP^+ cells were sorted by FACS and subjected to TIDE analysis. KKH *Sa*Cas9-edited iPSC mixtures and single clones were differentiated into cardiomyocytes, as previously described.[15]

Calcium imaging

Calcium imaging was performed as previously described.[41] iPSC-derived cardiomyocytes were replated on glass surfaces at single-cell density and loaded with the fluorescent calcium indicator Fluo-4 AM (Thermo Fisher) at 2 μM. Spontaneous calcium transients of beating iPSC-derived cardiomyocytes were imaged at 37°C using a Nikon A1R+ confocal system. Calcium transients were processed using Fiji software and analyzed using Microsoft Excel and Clampfit 10.7 software (Axon Instruments). The calcium-release phase was represented with time to peak, which was calculated as the time from baseline to maximal point of the transient. The calcium-reuptake phase was represented with the time constant tau by fitting the decay phase of calcium transients with a first-order exponential function.

In vivo AAV delivery into ΔEx50 mice

The ΔEx50 DMD mouse model was developed by deleting the mouse *Dmd* exon 50 using CRISPR/Cas9-mediated mutagenesis.[11] P4 ΔEx50 mice were injected intraperitoneally with 80 μL of AAV9 containing 2×10^{14} (low dose) or 4×10^{14} vg/kg (high dose) of All-In-One AAV9-KKH-*Sa*Cas9-sgRNAs using an ultrafine BD insulin syringe (Becton Dickinson). Four weeks after systemic delivery, ΔEx50 mice and WT littermates were dissected for physiological, biochemical, and histological analysis. Animal work described in this manuscript has been approved and conducted under the oversight of the University of Texas Southwestern Institutional Animal Care and Use Committee.

Genomic DNA and RNA isolation, cDNA synthesis, and PCR amplification

Genomic DNA of *DMD* ΔEx48–50 iPSCs, skeletal muscles and hearts of ΔEx50 mice was isolated using DirectPCR (cell) lysis reagent (Viagen Biotech) according to the manufacturer's protocol. Total RNA of skeletal muscles and heart of ΔEx50 mice was isolated using miRNeasy (QIAGEN) according to the manufacturer's protocol. cDNA was reverse-transcribed from total RNA using iScript Reverse Transcription Supermix (Bio-Rad Laboratories) according to the manufacturer's protocol. Genomic DNA and cDNA was PCR amplified using LongAmp *Taq* DNA polymerase (New England BioLabs) PCR products were sequenced and analyzed by TIDE analysis.[42] Primer sequences are listed in Table S1.

Amplicon deep-sequencing analysis of genomic DNA

PCR of genomic DNA was performed using primers designed against the human *DMD* exon 51, off-target sites, and mouse *Dmd* exon 51. A second round of PCR was performed to add Illumina flow cell binding sequence and barcodes. All primer sequences are listed in Table S1. Deep sequencing and data analysis were performed as previously described.[11]

Dystrophin immunocytochemistry and immunohistochemistry

Dystrophin immunocytochemistry was performed as previously described.[40] Primary antibodies used in immunocytochemistry were mouse anti-dystrophin antibody (MANDYS8, Sigma-Aldrich, D8168) and rabbit anti-troponin I antibody (H170, Santa Cruz Biotechnology). Secondary antibodies used in immunocytochemistry were biotinylated horse anti-mouse immunoglobulin G (IgG) (BMK-2202, Vector Laboratories) and fluorescein-conjugated donkey anti-rabbit IgG (Jackson ImmunoResearch). Skeletal muscles and heart were cryosectioned into 8-μm transverse sections. Immunohistochemistry was performed as previously described.[16] Antibodies used in immunohistochemistry were mouse anti-dystrophin antibody (MANDYS8, Sigma-Aldrich, D8168) and mouse on mouse biotinylated anti-mouse IgG (BMK-2202, Vector Laboratories).

Dystrophin western blot analysis

For western blot of iPSC-derived cardiomyocytes, 4×10^6 cells were lysed in lysis buffer (10% SDS, 62.5 mM tris [pH 6.8], 1 mM EDTA, and protease inhibitor). Heart and skeletal muscles were crushed into fine powder using a liquid-nitrogen-frozen crushing apparatus and lysed in the same lysis buffer as iPSC-derived cardiomyocytes. A total 50 μg of protein was loaded onto 4%–20% Criterion TGX Precast Midi Protein Gel (Bio-Rad Laboratories). Details of western blot running, transferring, and developing were previously described.[15] Primary antibodies used in western blot were mouse anti-dystrophin antibody (MANDYS8, Sigma-Aldrich, D8168) and mouse anti-vinculin antibody (Sigma-Aldrich, V9131). Secondary antibody used in western blot was goat anti-mouse horseradish peroxidase (HRP) antibody (Bio-Rad Laboratories).

Electrophysiological analysis of isolated EDL and soleus muscles

Four weeks after systemic All-In-One AAV9-KKH-*Sa*Cas9-sgRNAs gene editing, soleus, and EDL muscles of ΔEx50 mice and WT littermates were isolated for electrophysiological analysis. In brief, soleus and EDL muscles were surgically isolated from 4-week-old ΔEx50 mice, mounted on Grass FT03.C force transducers, bathed in physiological salt solution at 37°C, and gassed continuously with 95% O_2–5% CO_2. After calibration, muscles were adjusted to initial length at which the passive force was 0.5 g and then stimulated with two platinum-wire electrodes to establish optimal length (Lo) for obtaining maximal isometric tetanic tension step by step following the protocol (at 150 Hz for 2 s). Specific force (mN/mm^2) was calculated by normalizing contraction force to muscle cross-sectional area.

Statistics

All data are shown as means ± SEM. Unpaired two-tailed Student's t tests was performed to analyze Figure 1D and Figures S13C and S13D; two-way analysis of variance (ANOVA) with post hoc Tukey's multiple-comparisons test was performed to analyze Figure 4B; Brown-Forsythe and Welch ANOVA test was performed to analyze Figures 5A and 5B; nonlinear regression with extra sum-of-squares F test was performed to analyze Figures 5E and 5F; one-way ANOVA with post hoc Tukey's multiple-comparisons test was performed to analyze the rest of data. A $p < 0.05$ value was considered statistically significant. Data analyses were performed with GraphPad Prism software.

Data and materials availability

All data needed to evaluate the conclusions in the paper are present in the paper and/or the supplemental information. Additional data related to this paper may be requested from the authors.

SUPPLEMENTAL INFORMATION

Supplemental information can be found online at https://doi.org/10.1016/j.omtm.2021.05.014.

ACKNOWLEDGMENTS

We thank J. Cabrera for graphics, Y. Zhang and the Boston Children's Hospital Viral Core for AAV production, the Metabolic Phenotyping Core for serum CK analysis, the Sanger Sequencing Core and the Next Generation Sequencing Core for sequencing services, the Flow Cytometry Core for cell sorting, and the Histology Core for H&E staining. We are grateful to S. Hauschka (University of Washington) for providing the muscle-specific CK8e promoter. This work was supported by the NIH (grant HL130253), the Senator Paul D. Wellstone Muscular Dystrophy Specialized Research Center (grant P50 HD 087351), and the Robert A. Welch Foundation (grant 1-0025 to E.N.O.).

AUTHOR CONTRIBUTIONS

Y.Z., R.B.-D., and E.N.O. wrote and edited the manuscript. Y.Z. designed the experiments, cloned AAV constructs, and performed iPSC culture, animal studies, tissue cryosectioning, imaging, and data analysis. T.N. performed iPSC culture, western blot, and immunocytochemistry. H.L. performed genomic PCR, RT-PCR, and data analysis. J.H. performed the muscle electrophysiology analysis. A.A. performed cardiomyocyte calcium analysis. E.S.-O. performed immunohistochemistry, western blot, and imaging. Z.W. performed deep-sequencing analysis. A.A.M. performed grip-strength analysis, animal dissection, and tissue-processing experiments. P.P.A.M. provided oversight of the electrophysiology analysis.

DECLARATION OF INTERESTS

R.B.-D and E.N.O. are consultants for Vertex Therapeutics. The other authors declare that they have no competing interests.

REFERENCES

1. Hoffman, E.P., Brown, R.H., Jr., and Kunkel, L.M. (1987). Dystrophin: the protein product of the Duchenne muscular dystrophy locus. Cell *51*, 919–928.
2. Koenig, M., Hoffman, E.P., Bertelson, C.J., Monaco, A.P., Feener, C., and Kunkel, L.M. (1987). Complete cloning of the Duchenne muscular dystrophy (DMD) cDNA and preliminary genomic organization of the DMD gene in normal and affected individuals. Cell *50*, 509–517.
3. Gao, Q.Q., and McNally, E.M. (2015). The Dystrophin Complex: Structure, Function, and Implications for Therapy. Compr. Physiol. *5*, 1223–1239.
4. Guiraud, S., Aartsma-Rus, A., Vieira, N.M., Davies, K.E., van Ommen, G.J., and Kunkel, L.M. (2015). The Pathogenesis and Therapy of Muscular Dystrophies. Annu. Rev. Genomics Hum. Genet. *16*, 281–308.
5. Cong, L., Ran, F.A., Cox, D., Lin, S., Barretto, R., Habib, N., Hsu, P.D., Wu, X., Jiang, W., Marraffini, L.A., and Zhang, F. (2013). Multiplex genome engineering using CRISPR/Cas systems. Science *339*, 819–823.
6. Jinek, M., Chylinski, K., Fonfara, I., Hauer, M., Doudna, J.A., and Charpentier, E. (2012). A programmable dual-RNA-guided DNA endonuclease in adaptive bacterial immunity. Science *337*, 816–821.
7. Mali, P., Yang, L., Esvelt, K.M., Aach, J., Guell, M., DiCarlo, J.E., Norville, J.E., and Church, G.M. (2013). RNA-guided human genome engineering via Cas9. Science *339*, 823–826.
8. Iyer, S., Suresh, S., Guo, D., Daman, K., Chen, J.C.J., Liu, P., Zieger, M., Luk, K., Roscoe, B.P., Mueller, C., et al. (2019). Precise therapeutic gene correction by a simple nuclease-induced double-stranded break. Nature *568*, 561–565.
9. Gallagher, D.N., and Haber, J.E. (2018). Repair of a Site-Specific DNA Cleavage: Old-School Lessons for Cas9-Mediated Gene Editing. ACS Chem. Biol. *13*, 397–405.
10. Amoasii, L., Hildyard, J.C.W., Li, H., Sanchez-Ortiz, E., Mireault, A., Caballero, D., Harron, R., Stathopoulou, T.R., Massey, C., Shelton, J.M., et al. (2018). Gene editing restores dystrophin expression in a canine model of Duchenne muscular dystrophy. Science *362*, 86–91.
11. Amoasii, L., Long, C., Li, H., Mireault, A.A., Shelton, J.M., Sanchez-Ortiz, E., McAnally, J.R., Bhattacharyya, S., Schmidt, F., Grimm, D., et al. (2017). Single-cut genome editing restores dystrophin expression in a new mouse model of muscular dystrophy. Sci. Transl. Med. *9*, eaan8081.
12. Bengtsson, N.E., Hall, J.K., Odom, G.L., Phelps, M.P., Andrus, C.R., Hawkins, R.D., Hauschka, S.D., Chamberlain, J.R., and Chamberlain, J.S. (2017). Muscle-specific CRISPR/Cas9 dystrophin gene editing ameliorates pathophysiology in a mouse model for Duchenne muscular dystrophy. Nat. Commun. *8*, 14454.
13. Hakim, C.H., Wasala, N.B., Nelson, C.E., Wasala, L.P., Yue, Y., Louderman, J.A., Lessa, T.B., Dai, A., Zhang, K., Jenkins, G.J., et al. (2018). AAV CRISPR editing rescues cardiac and muscle function for 18 months in dystrophic mice. JCI Insight *3*, 124297.
14. Long, C., Amoasii, L., Mireault, A.A., McAnally, J.R., Li, H., Sanchez-Ortiz, E., Bhattacharyya, S., Shelton, J.M., Bassel-Duby, R., and Olson, E.N. (2016). Postnatal genome editing partially restores dystrophin expression in a mouse model of muscular dystrophy. Science *351*, 400–403.
15. Min, Y.L., Chemello, F., Li, H., Rodriguez-Caycedo, C., Sanchez-Ortiz, E., Mireault, A.A., McAnally, J.R., Shelton, J.M., Zhang, Y., Bassel-Duby, R., and Olson, E.N. (2020). Correction of Three Prominent Mutations in Mouse and Human Models of Duchenne Muscular Dystrophy by Single-Cut Genome Editing. Mol. Ther. *28*, 2044–2055.
16. Min, Y.L., Li, H., Rodriguez-Caycedo, C., Mireault, A.A., Huang, J., Shelton, J.M., McAnally, J.R., Amoasii, L., Mammen, P.P.A., Bassel-Duby, R., and Olson, E.N. (2019). CRISPR-Cas9 corrects Duchenne muscular dystrophy exon 44 deletion mutations in mice and human cells. Sci. Adv. *5*, eaav4324.
17. Nelson, C.E., Hakim, C.H., Ousterout, D.G., Thakore, P.I., Moreb, E.A., Castellanos Rivera, R.M., Madhavan, S., Pan, X., Ran, F.A., Yan, W.X., et al. (2016). In vivo genome editing improves muscle function in a mouse model of Duchenne muscular dystrophy. Science *351*, 403–407.
18. Nelson, C.E., Wu, Y., Gemberling, M.P., Oliver, M.L., Waller, M.A., Bohning, J.D., Robinson-Hamm, J.N., Bulaklak, K., Castellanos Rivera, R.M., Collier, J.H., et al. (2019). Long-term evaluation of AAV-CRISPR genome editing for Duchenne muscular dystrophy. Nat. Med. *25*, 427–432.
19. Tabebordbar, M., Zhu, K., Cheng, J.K.W., Chew, W.L., Widrick, J.J., Yan, W.X., Maesner, C., Wu, E.Y., Xiao, R., Ran, F.A., et al. (2016). In vivo gene editing in dystrophic mouse muscle and muscle stem cells. Science *351*, 407–411.

20. Zhang, Y., Li, H., Min, Y.L., Sanchez-Ortiz, E., Huang, J., Mireault, A.A., Shelton, J.M., Kim, J., Mammen, P.P.A., Bassel-Duby, R., and Olson, E.N. (2020). Enhanced CRISPR-Cas9 correction of Duchenne muscular dystrophy in mice by a self-complementary AAV delivery system. Sci. Adv. *6*, eaay6812.

21. Amoasii, L., Li, H., Zhang, Y., Min, Y.L., Sanchez-Ortiz, E., Shelton, J.M., Long, C., Mireault, A.A., Bhattacharyya, S., McAnally, J.R., et al. (2019). In vivo non-invasive monitoring of dystrophin correction in a new Duchenne muscular dystrophy reporter mouse. Nat. Commun. *10*, 4537.

22. Kwon, J.B., Ettyreddy, A.R., Vankara, A., Bohning, J.D., Devlin, G., Hauschka, S.D., Asokan, A., and Gersbach, C.A. (2020). *In Vivo* Gene Editing of Muscle Stem Cells with Adeno-Associated Viral Vectors in a Mouse Model of Duchenne Muscular Dystrophy. Mol. Ther. Methods Clin. Dev. *19*, 320–329.

23. Kleinstiver, B.P., Prew, M.S., Tsai, S.Q., Nguyen, N.T., Topkar, V.V., Zheng, Z., and Joung, J.K. (2015). Broadening the targeting range of Staphylococcus aureus CRISPR-Cas9 by modifying PAM recognition. Nat. Biotechnol. *33*, 1293–1298.

24. Aartsma-Rus, A., Fokkema, I., Verschuuren, J., Ginjaar, I., van Deutekom, J., van Ommen, G.J., and den Dunnen, J.T. (2009). Theoretic applicability of antisense-mediated exon skipping for Duchenne muscular dystrophy mutations. Hum. Mutat. *30*, 293–299.

25. Himeda, C.L., Chen, X., and Hauschka, S.D. (2011). Design and testing of regulatory cassettes for optimal activity in skeletal and cardiac muscles. Methods Mol. Biol. *709*, 3–19.

26. Chemello, F., Bassel-Duby, R., and Olson, E.N. (2020). Correction of muscular dystrophies by CRISPR gene editing. J. Clin. Invest. *130*, 2766–2776.

27. Min, Y.L., Bassel-Duby, R., and Olson, E.N. (2019). CRISPR Correction of Duchenne Muscular Dystrophy. Annu. Rev. Med. *70*, 239–255.

28. Zhang, Y., Long, C., Bassel-Duby, R., and Olson, E.N. (2018). Myoediting: Toward Prevention of Muscular Dystrophy by Therapeutic Genome Editing. Physiol. Rev. *98*, 1205–1240.

29. Zuo, Z., and Liu, J. (2016). Cas9-catalyzed DNA Cleavage Generates Staggered Ends: Evidence from Molecular Dynamics Simulations. Sci. Rep. *5*, 37584.

30. Lemos, B.R., Kaplan, A.C., Bae, J.E., Ferrazzoli, A.E., Kuo, J., Anand, R.P., Waterman, D.P., and Haber, J.E. (2018). CRISPR/Cas9 cleavages in budding yeast reveal templated insertions and strand-specific insertion/deletion profiles. Proc. Natl. Acad. Sci. USA *115*, E2040–E2047.

31. Shen, M.W., Arbab, M., Hsu, J.Y., Worstell, D., Culbertson, S.J., Krabbe, O., Cassa, C.A., Liu, D.R., Gifford, D.K., and Sherwood, R.I. (2018). Predictable and precise template-free CRISPR editing of pathogenic variants. Nature *563*, 646–651.

32. Yin, H., Price, F., and Rudnicki, M.A. (2013). Satellite cells and the muscle stem cell niche. Physiol. Rev. *93*, 23–67.

33. Nance, M.E., Shi, R., Hakim, C.H., Wasala, N.B., Yue, Y., Pan, X., Zhang, T., Robinson, C.A., Duan, S.X., Yao, G., et al. (2019). AAV9 Edits Muscle Stem Cells in Normal and Dystrophic Adult Mice. Mol. Ther. *27*, 1568–1585.

34. Duan, D. (2018). Systemic AAV Micro-dystrophin Gene Therapy for Duchenne Muscular Dystrophy. Mol. Ther. *26*, 2337–2356.

35. Truong, D.J., Kühner, K., Kühn, R., Werfel, S., Engelhardt, S., Wurst, W., and Ortiz, O. (2015). Development of an intein-mediated split-Cas9 system for gene therapy. Nucleic Acids Res. *43*, 6450–6458.

36. Chew, W.L., Tabebordbar, M., Cheng, J.K., Mali, P., Wu, E.Y., Ng, A.H., Zhu, K., Wagers, A.J., and Church, G.M. (2016). A multifunctional AAV-CRISPR-Cas9 and its host response. Nat. Methods *13*, 868–874.

37. Hoffman, E.P., Kunkel, L.M., Angelini, C., Clarke, A., Johnson, M., and Harris, J.B. (1989). Improved diagnosis of Becker muscular dystrophy by dystrophin testing. Neurology *39*, 1011–1017.

38. Chemello, F., Chai, A.C., Li, H., Rodriguez-Caycedo, C., Sanchez-Ortiz, E., Atmanli, A., Mireault, A.A., Liu, N., Bassel-Duby, R., and Olson, E.N. (2021). Precise correction of Duchenne muscular dystrophy exon deletion mutations by base and prime editing. Sci. Adv. *7*, eabg4910.

39. Ran, F.A., Cong, L., Yan, W.X., Scott, D.A., Gootenberg, J.S., Kriz, A.J., Zetsche, B., Shalem, O., Wu, X., Makarova, K.S., et al. (2015). In vivo genome editing using Staphylococcus aureus Cas9. Nature *520*, 186–191.

40. Zhang, Y., Long, C., Li, H., McAnally, J.R., Baskin, K.K., Shelton, J.M., Bassel-Duby, R., and Olson, E.N. (2017). CRISPR-Cpf1 correction of muscular dystrophy mutations in human cardiomyocytes and mice. Sci. Adv. *3*, e1602814.

41. Atmanli, A., Hu, D., Deiman, F.E., van de Vrugt, A.M., Cherbonneau, F., Black, L.D., 3rd, and Domian, I.J. (2019). Multiplex live single-cell transcriptional analysis demarcates cellular functional heterogeneity. eLife *8*, e49599.

42. Brinkman, E.K., Chen, T., Amendola, M., and van Steensel, B. (2014). Easy quantitative assessment of genome editing by sequence trace decomposition. Nucleic Acids Res. *42*, e168.